Science Journal of Circuits, Systems and Signal Processing
2014; 3(6): 35-46
Published online January 16, 2015 (http://www.sciencepublishinggroup.com/j/cssp)
doi: 10.11648/j.cssp.20140306.11
ISSN: 2326-9065 (Print); ISSN: 2326-9073 (Online)

Non-separable 3D integer wavelet transform for lossless data compression

Teerapong Orachon[1, *], Suvit Poomrittigul[2], Taichi Yoshida[1], Masahiro Iwahashi[1], Somchart Chokchaitam[3]

[1]Department of Electrical Engineering, Nagaoka University of Technology, Nagaoka, Japan
[2]Department of Computer Technology, Pathumwan Institute of Technology, Bangkok, Thailand
[3]Department of Electrical Engineering, Thammasat University, Bangkok, Thailand

Email address:
oteerapong@gmail.com (T. Orachon), suvitp@gmail.com (S. Poomrittigul)

To cite this article:
Teerapong Orachon, Suvit Poomrittigul, Taichi Yoshida, Masahiro Iwahashi, Somchart Chokchaitam. Non-Separable 3D Integer Wavelet Transform for Lossless Data Compression. *Science Journal of Circuits, Systems and Signal Processing.* Vol. 3, No. 6, 2014, pp. 35-46.
doi: 10.11648/j.cssp.20140306.11

Abstract: This paper proposes a three-dimensional (3D) integer wavelet transform with reduced amount of rounding noise. Non-separable multi-dimensional lifting structures are introduced to decrease the total number of lifting steps. Since the lifting step contains a rounding operation, variance of the rounding noise generated due to the rounding operation inside the transform is reduced. This paper also investigates performance of the transform from various aspects such as 1) variance of the noise in frequency domain and those in pixel domain, 2) the rate distortion curve in lossy coding mode and the entropy rate in lossless coding mode, 3) computational time of the transforms, and 4) feature comparison with other methods. The proposed wavelet transform has a merit that its output signal, apart from the rounding noise, is exactly the same as the conventional separable structure which is a cascade of 1D structure. Due to this compatibility, it becomes possible to utilize legacy of previously designed 1D wavelet transforms with preferable properties such as the regularity. Furthermore, total amount of the rounding noise which is generated due to integer expression of signal values inside the transform is significantly reduced. This is because the total number of rounding operations is decreased by introducing the non-separable multi-dimensional lifting structure which includes multi-dimensional memory accessing. It contributes to increase coding performance of a system based on the 3D wavelet transform. As a result of experiments, it was observed that the proposed method increases performance of data compression of various 3D input signals.

Keywords: Wavelet, Transform, Lifting, 3D, Rounding, Coding

1. Introduction

Over the past few decades, quality of image signals have been dramatically increased in respect of pixel resolution, frame rate and dynamic range of pixel values. The more the quality increases, the more data volume becomes. Therefore image compression techniques based on a transform have been playing an important role for storage and communications of digital media data.

For still images, a two-dimensional (2D) transform such as the discrete cosine transform (DCT) and the wavelet transform has been utilized. Recently, various types of three-dimensional (3D) transforms have been investigated for video, hyper spectral images, integral images and medical volumetric data [1-4]. This paper deals with a '3D' wavelet transform with reduced amount of rounding noise inside the transform for high performance 'lossless' data compression.

So far, a class of 'separable'2D wavelet transform has been widely developed for various applications. The JPEG 2000 international standard also adopts this class of transform [5, 6]. It has been applied for digital cinema [7, 8]. Since its transfer function is composed of a product of the horizontal 1D transfer function and the vertical one, it can inherit legacy of previously designed 1D structure suitable for hardware implementations [9-11]. It can also have the regularity and low sensitivity to various noises [12, 13]. However, most of them are designed for 'lossy' coding of images for practically reasonable data compression rate.

For 'lossless' coding of images, it is necessary to have transformed values as integers for entropy coding, and also inversely transform them to reconstruct the original integer pixel values without any loss. It has been implemented in the lifting structure with rounding operations as the integer wavelet transform and extended based on the international standard [14, 15]. The radar network has also been utilized for the reversible color transform and the integer DCT [16-22].

Those are indeed 'lossless'. A set of forward and backward transform guarantees lossless reconstruction of the original integer pixel values. However, there exist 'rounding noise' just after the forward transform. To reduce those noise due to the rounding operations applied at each of the lifting steps, a 'non-separable' structure was introduced to decrease the total number of lifting steps as well as the rounding operations [23].

Most of the non-separable structures have been initially introduced to increase precision of the prediction by adapting to local context of neighboring pixels [24-26]. More general designing problem based on a sparse criteria has been investigated [27]. Recently, directionality has been utilized in a generalized poly-phase representation [28, 29]. Those have been focusing on designing adaptive high pass filters of the wavelet transform.

A new class of non-separable 2D structure has been reported in [30-33]. Its transfer function can be expressed as a product of 1D function. In this sense, the transform based on this structure is 'compatible' to the separable transform. However, in its implementation, it is not a cascade of 1D signal processing in the 1D structure. It requires multi-dimensional memory accessing. In addition, those are not adaptive to local context of pixels. Even though it has some drawbacks yet, it has advantage that it decreases the total number of lifting steps as well as the rounding operations.

Unlike those previous studies on the 2D case, this paper proposes a '3D' integer wavelet transform for 'lossless' coding of 3D signals with reduced amount of the rounding noise. In a conference paper [34], a non-separable 3D lifting structure was introduced to decrease the total number of lifting steps. However its computational complexity becomes huge since it requires 3D memory accessing. In case of video signal processing, it requires inter-frame memory accessing. Therefore it costs huge memory space. Therefore this paper newly introduces non-separable 2D structures to construct the 3D integer wavelet transform.

In addition, investigation in [34] on performance of the 3D integer wavelet transform was limited to noise variance in frequency domain only. Its input signal was also limited to only one MRI data set. Therefore this paper clarifies not only 1) variance of the noise in frequency domain and those in pixel domain, but also 2) the rate distortion curve in lossy coding mode and the entropy rate in lossless coding mode, 3) computational time of the transforms, and 4) feature comparison with other methods. In addition to the MRI data set, various kinds of input data are tested in this paper.

The proposed wavelet transform has a merit that its output signals, apart from the rounding noise, are exactly the same as a conventional transform whose transfer function is expressed as a product of 1D transfer functions. Due to this compatibility, it becomes possible to utilize legacy of previously designed 1D wavelet transforms. Furthermore, total amount of the rounding noise is significantly reduced. It contributes to increase coding performance of data compression system based on the 3D wavelet transform.

This paper is organized as follows. The reason why the non-separable structure reduces the lifting steps is explained in 2. Discussion is extended to 3D case in 3. Non-separable 2D structures for the 3D wavelet transform is newly introduced in 4. The non-separable multi-dimensional structures are compared in various aspects for various input signals in 5. This paper is concluded in 6.

2. Wavelet Transform and Lifting Structure

It is explained how the rounding noise is reduced introducing a non-separable 2D structure.

2.1. One-Dimensional (1D) Wavelet Transform

Fig.1 illustrates a one-dimensional (1D) integer wavelet transform for lossless coding of discrete 1D signal. In encoding side, the input signal X is fed into the forward transform which outputs low frequency band signal Y_L and high frequency band signal Y_H. Each of them are coded with an entropy encoder to generate a bit stream for storage and communications. In decoding side, the band signals are decoded and inversely transformed.

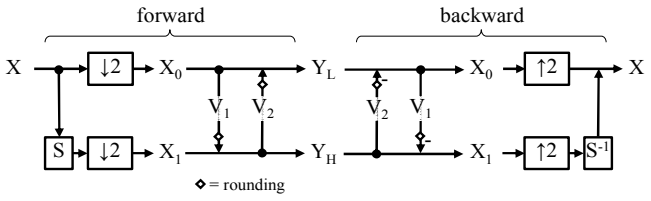

Figure 1. *One-dimensional (1D) integer wavelet transform.*

This system is referred to as the 'integer' wavelet transform for 'lossless' coding since it reconstructs the original signal X without any loss. This is because all the signal values inside the transform are rounded to integers, and the rounding noise generated by the rounding operation is canceled at the output of the backward transform.

In detail, the original signal X given in integer values with length $N$is split into two half-length sequences X_0 and X_1 as

$$\begin{cases} x_0(m) = x(2m) \\ x_1(m) = x(2m+1) \end{cases} \tag{1}$$

for m=0,1,…,M-1 where

$$\begin{cases} X = [\, x(0) \quad x(1) \quad \cdots \quad x(N-1)] \\ X_0 = [x_0(0) \quad x_0(1) \quad \cdots \quad x_0(M-1)] \\ X_1 = [\, x_1(0) \quad x_1(1) \quad \cdots \quad x_1(M-1)] \end{cases} \tag{2}$$

and $M=N/2$. In the 1st lifting step, X_1 is predicted from X_0 as

$$y_H(m) = x_1(m) + R[V_1 * x_0(m)] \tag{3}$$

where $R[x]$ denotes an integer rounded from the original value x, and V_1* denotes convolution. The convolution is defined as

$$V_1 * x_0(m) = h_1\left(x_0(m) + x_0(m+1)\right) \tag{4}$$

where h_1 is a filter coefficient. In the 2nd lifting step, X_0 is updated from Y_H as

$$y_L(m) = x_0(m) + R[V_2 * y_H(m)] \tag{5}$$

where the convolution V_2* is defined as

$$V_2 * y_H(m) = h_2\left(y_H(m) + y_H(m-1)\right) \tag{6}$$

where h_2 is a filter coefficient. As the rounding operations $R[\cdot]$ are applied, all the signal values are expressed as integers inside this integer wavelet transform.

In the lifting wavelet transforms, filter coefficients have been carefully determined in previous reports. For example, a set (h_1, h_2) = (-1/2,1/4) is utilized in JPEG 2000 international standard [5,6]. In this case, a low pass filter of the forward transform has unity gain for a constant signal, and zero gain for an alternating signal. Those properties are expressed as

$$\begin{aligned} y_L(m) &= x_0(m) + h_2\left(y_H(m) + y_H(m-1)\right) \\ &= \begin{cases} \text{constant} & for \quad x(n) = \text{constant} \\ 0 & for \quad x(n) = (-1)^n \end{cases} \end{aligned} \tag{7}$$

and a high pass filter has

$$\begin{aligned} y_H(m) &= x_1(m) + h_1\left(x_0(m) + x_0(m+1)\right) \\ &= x(2m+1) + h_1\left(x(2m) + x(2m+2)\right) \\ &= 0 \quad for \quad x(n) = \text{constant}. \end{aligned} \tag{8}$$

It is desirable to utilize good properties like (7) and (8), and other properties such as the vanishing moment in designing a multi-dimensional transform.

2.2. Two-Dimensional (2D) Wavelet Transform

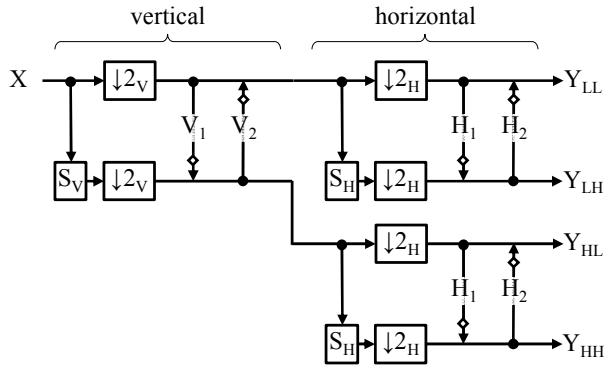

Figure 2. *Two-dimensional (2D) integer wavelet transform.*

Fig.2 illustrates a two-dimensional (2D) integer wavelet transform. In this transform, the 1D transform is applied vertically to the 2D input image X. Next, the same 1D transform is applied horizontally. As a result, 4 frequency band signals Y_{LL}, Y_{LH}, Y_{HL} and Y_{HH} are generated. Since this transform is a product of 1D transforms, it is referred to as the 'separable' transform.

Fig. 3 illustrates another expression of Fig. 2. It outputs the same band signals to those in Fig. 2. It splits the 2D input signal x (n_1,n_2) into 4 groups as

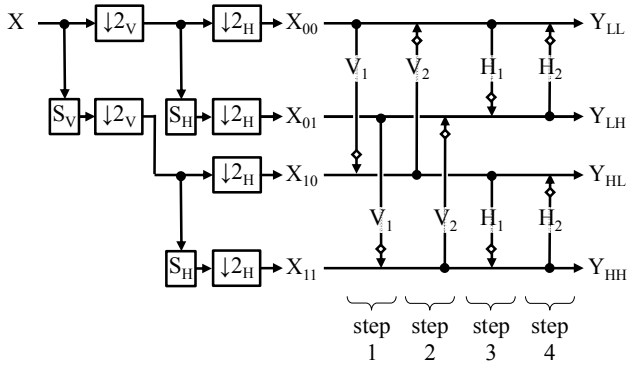

Figure 3. *Separable 2D structure for 2D wavelet transform.*

$$\begin{cases} x_{00}(m_1,m_2) = x(2m_1 \quad , 2m_2 \quad) \\ x_{10}(m_1,m_2) = x(2m_1+1, 2m_2 \quad) \\ x_{01}(m_1,m_2) = x(2m_1 \quad , 2m_2+1) \\ x_{11}(m_1,m_2) = x(2m_1+1, 2m_2+1) \end{cases} \tag{9}$$

where m_1=0,1,…,M_1-1and m_2=0,1,…,M_2-1 for $M_1=N_1/2$ and $M_2=N_2/2$. In the 1st lifting step, X_{10} and X_{11} are predicted from X_{00} and X_{01} respectively as

$$\begin{cases} x_{10}^{(1)}(m_1,m_2) = x_{10}(m_1,m_2) + R[V_1 * x_{00}(m_1,m_2)] \\ x_{11}^{(1)}(m_1,m_2) = x_{11}(m_1,m_2) + R[V_1 * x_{01}(m_1,m_2)] \end{cases} \tag{10}$$

where

$$\begin{cases} V_1 * x_{00}(m_1,m_2) = h_1\left(x_{00}(m_1,m_2) + x_{00}(m_1+1,m_2)\right) \\ V_1 * x_{01}(m_1,m_2) = h_1\left(x_{01}(m_1,m_2) + x_{01}(m_1+1,m_2)\right). \end{cases} \tag{11}$$

This convolution is performed vertically along with the variable m_1. Similarly, in the 2nd lifting step, X_{00} and X_{01} are updated from X_{10} and X_{11} respectively as

$$\begin{cases} x_{00}^{(2)}(m_1,m_2) = x_{00}(m_1,m_2) + R[V_2 * x_{10}^{(1)}(m_1,m_2)] \\ x_{01}^{(2)}(m_1,m_2) = x_{01}(m_1,m_2) + R[V_2 * x_{11}^{(1)}(m_1,m_2)] \end{cases} \tag{12}$$

where

$$\begin{cases} V_2 * x_{10}^{(1)}(m_1,m_2) = h_2\left(x_{10}^{(1)}(m_1,m_2) + x_{10}^{(1)}(m_1-1,m_2)\right) \\ V_2 * x_{11}^{(1)}(m_1,m_2) = h_2\left(x_{11}^{(1)}(m_1,m_2) + x_{11}^{(1)}(m_1-1,m_2)\right). \end{cases} \tag{13}$$

In the 3rd and 4th lifting steps, the process is repeated

horizontally along with the variable m_2. For example, the horizontal convolutions are given as

$$\begin{cases} H_1 * x_{00}^{(2)}(m_1,m_2) = h_1\left(x_{00}^{(2)}(m_1,m_2) + x_{00}^{(2)}(m_1,m_2+1)\right) \\ H_2 * x_{01}^{(3)}(m_1,m_2) = h_2\left(x_{01}^{(3)}(m_1,m_2) + x_{01}^{(3)}(m_1,m_2-1)\right) \end{cases} \quad (14)$$

Note that this 'separable' 2D lifting structure has 8 rounding operations in total since each of 8 lifting step has one rounding operation. Those are source of the rounding noise to be reduced by introducing a non-separable structure in this paper.

2.3. Non-separable 2D Structure

Fig. 4 illustrates a 'non-separable' 2D lifting structure. Different from the separable stricture, it has multi-input single-output lifting steps. In addition, it has less lifting steps comparing to the separable one. Therefore it has less rounding operations as well as rounding noise. Comparing to Fig.3, the total number of lifting steps is reduced from 4 to 3 (75 %), and the total number of rounding operations is reduced from 8 to 4 (50 %) in Fig.4. It also reduces the total amount of rounding noise [33]. Note that this transform has the properties of the 1D structure in (7) and (8) since its transfer function is the same as that of the 'separable' transform in 2.2.

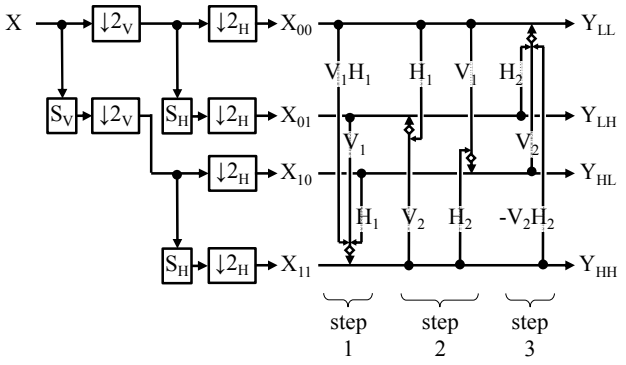

Figure 4. *Non-separable 2D structure for 2D wavelet transform.*

In detail, the 1st lifting step predicts X_{11} from multi-inputs X_{00}, X_{01} and X_{10} as

$$\begin{aligned} y_{HH}(\mathbf{m}) = x_{11}(\mathbf{m}) + R[\, & V_1 * H_1 * x_{00}(\mathbf{m}) \\ & + V_1 * x_{01}(\mathbf{m}) + H_1 * x_{10}(\mathbf{m})\,] \end{aligned} \quad (15)$$

for (m)=(m_1, m_2). In this prediction, a diagonal prediction

$$\begin{aligned} V_1 * H_1 * x_{00}(\mathbf{m}) = h_1 h_1\big(& x_{00}(m_1,m_2) + x_{00}(m_1+1,m_2) \\ & + x_{00}(m_1,m_2+1) + x_{00}(m_1+1,m_2+1)\big) \end{aligned} \quad (16)$$

is utilized. In the 2nd lifting step, two predictions

$$y_{LH}(\mathbf{m}) = x_{01}(\mathbf{m}) + R[\, H_1 * x_{00}(\mathbf{m}) + V_2 * y_{HH}(\mathbf{m})\,] \quad (17)$$

and

$$y_{HL}(\mathbf{m}) = x_{10}(\mathbf{m}) + R[\, V_1 * x_{00}(\mathbf{m}) + H_2 * y_{HH}(\mathbf{m})\,] \quad (18)$$

are applied. Note that these two steps can be done simultaneously with a parallel processor sine it is not necessary to wait for calculation results each other. Finally, the 3rd lifting step completes the transform as

$$\begin{aligned} y_{LL}(\mathbf{m}) = x_{00}(\mathbf{m}) + R[\, & H_2 * y_{LH}(\mathbf{m}) \\ & + V_2 * y_{HL}(\mathbf{m}) - V_2 * H_2 * y_{HH}(\mathbf{m})\,]. \end{aligned} \quad (19)$$

As a result, this non-separable structure outputs the same band signals as the separable 2D transform apart from the rounding noise. It is referred to as 'compatibility'. In the next section, this theory is extended to 3D case.

3. Three-Dimensional (3D) Wavelet Transform

A 'non-separable' 3D structure is summarized after describing the 'separable' 3D structure.

3.1. Separable 3D Structure

Fig. 5 illustrates a 'separable'3D lifting structure. A 3D input signal X is split into 8 groups and single-input single-output lifting steps are applied to generate 8 frequency band signals. This structure has 6 lifting steps and 24 rounding operations. We are going to reduce these numbers in this paper.

In detail, the 3D input signal $x(n_1,n_2,n_3)$ is split into 8 groups as

$$\begin{cases} x_{000}(\mathbf{m}) = x(2m_1 \;\;, 2m_2 \;\;, 2m_3 \;\;) \\ x_{001}(\mathbf{m}) = x(2m_1 \;\;, 2m_2 \;\;, 2m_3+1) \\ x_{010}(\mathbf{m}) = x(2m_1 \;\;, 2m_2+1, 2m_3 \;\;) \\ x_{011}(\mathbf{m}) = x(2m_1 \;\;, 2m_2+1, 2m_3+1) \\ x_{100}(\mathbf{m}) = x(2m_1+1, 2m_2 \;\;, 2m_3 \;\;) \\ x_{101}(\mathbf{m}) = x(2m_1+1, 2m_2 \;\;, 2m_3+1) \\ x_{110}(\mathbf{m}) = x(2m_1+1, 2m_2+1, 2m_3 \;\;) \\ x_{111}(\mathbf{m}) = x(2m_1+1, 2m_2+1, 2m_3+1) \end{cases} \quad (20)$$

for (m)=(m_1,m_2,m_3).In the 1st lifting step, the vertical prediction is applied as

$$\begin{bmatrix} x_{100}^{(1)}(\mathbf{m}) \\ x_{101}^{(1)}(\mathbf{m}) \\ x_{110}^{(1)}(\mathbf{m}) \\ x_{111}^{(1)}(\mathbf{m}) \end{bmatrix} = \begin{bmatrix} x_{100}(\mathbf{m}) \\ x_{101}(\mathbf{m}) \\ x_{110}(\mathbf{m}) \\ x_{111}(\mathbf{m}) \end{bmatrix} + \begin{bmatrix} R[V_1 * x_{000}(\mathbf{m})] \\ R[V_1 * x_{001}(\mathbf{m})] \\ R[V_1 * x_{010}(\mathbf{m})] \\ R[V_1 * x_{011}(\mathbf{m})] \end{bmatrix} \quad (21)$$

where'$V_1 *$ ' denotes the vertical convolution along with the variable m_1 similar to (11). After the updating

$$\begin{bmatrix} x_{000}^{(2)}(\mathbf{m}) \\ x_{001}^{(2)}(\mathbf{m}) \\ x_{010}^{(2)}(\mathbf{m}) \\ x_{011}^{(2)}(\mathbf{m}) \end{bmatrix} = \begin{bmatrix} x_{000}(\mathbf{m}) \\ x_{001}(\mathbf{m}) \\ x_{010}(\mathbf{m}) \\ x_{011}(\mathbf{m}) \end{bmatrix} + \begin{bmatrix} R[V_2 * x_{100}^{(1)}(\mathbf{m})] \\ R[V_2 * x_{101}^{(1)}(\mathbf{m})] \\ R[V_2 * x_{110}^{(1)}(\mathbf{m})] \\ R[V_2 * x_{111}^{(1)}(\mathbf{m})] \end{bmatrix} \quad (22)$$

in the 2nd lifting step, the horizontal prediction

$$\begin{bmatrix} x_{010}^{(3)}(\mathbf{m}) \\ x_{011}^{(3)}(\mathbf{m}) \\ x_{000}^{(4)}(\mathbf{m}) \\ x_{001}^{(4)}(\mathbf{m}) \end{bmatrix} = \begin{bmatrix} x_{010}^{(2)}(\mathbf{m}) \\ x_{011}^{(2)}(\mathbf{m}) \\ x_{000}^{(2)}(\mathbf{m}) \\ x_{001}^{(2)}(\mathbf{m}) \end{bmatrix} + \begin{bmatrix} R[H_1 * x_{000}^{(2)}(\mathbf{m})] \\ R[H_1 * x_{001}^{(2)}(\mathbf{m})] \\ R[H_2 * x_{010}^{(3)}(\mathbf{m})] \\ R[H_2 * x_{011}^{(3)}(\mathbf{m})] \end{bmatrix} \quad (23)$$

is applied where '$H_1 *$ ' and '$H_2 *$ ' denote the horizontal convolution along with the variable m_2 similar to (14). In the 5th and 6th lifting steps, the convolution '$D_1 *$ ' and '$D_2 *$ ' are performed along with the variable m_3.

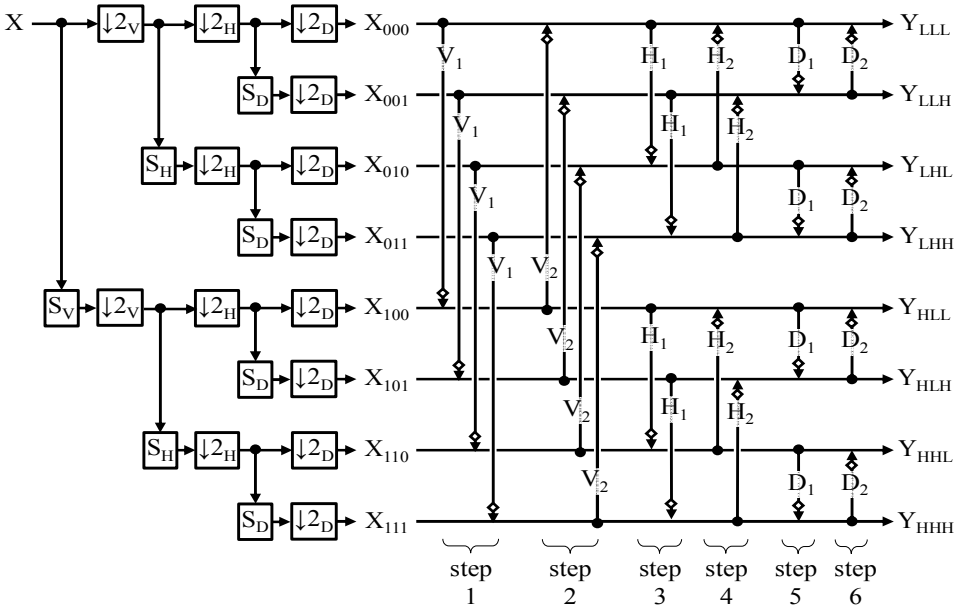

Figure 5. *Separable 3D structure 'Sep3D' for 3D wavelet transform.*

In this separable structure, the Nth lifting step must wait for calculation results of its previous N-1th lifting step. It increases delay from the input to the output. These lifting steps are reduced introducing non-separable structures composed of multi-dimensional memory accessing in the next subsection.

3.2. Non-separable 3D Structure

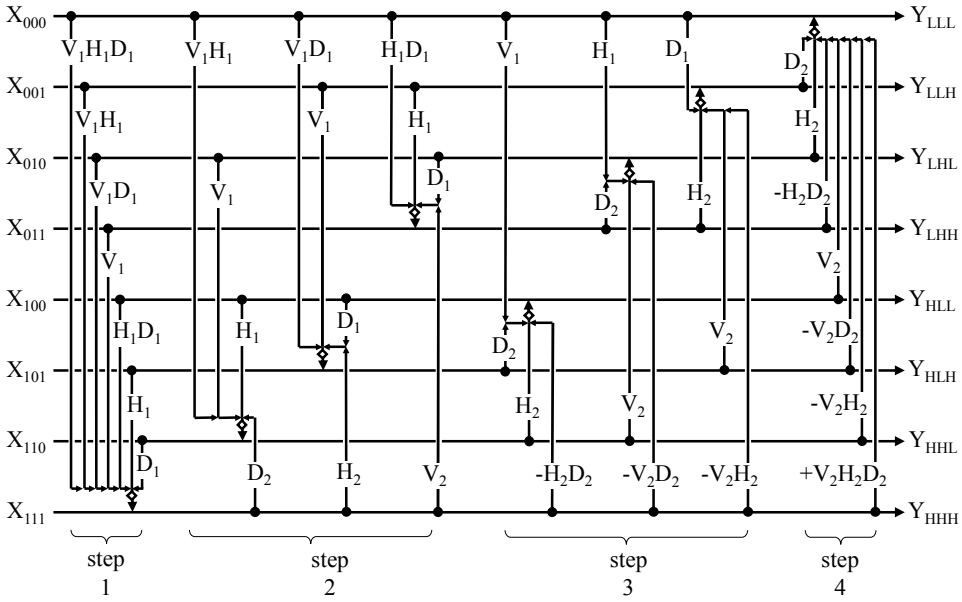

Figure 6. *Non-separable 3D structure 'Ns3D' for 3D wavelet transform.*

Fig. 6 illustrates the 'non-separable'3D lifting structure in [34]. In this structure, multi-input single-output lifting steps are introduced. It means 3D memory accessing. Comparing to the existing separable structure, the total number of lifting steps is reduced from 6 to 4 (66.7 %). Therefore it is expected to reduce the delay due to waiting for results of the previous

lifting step utilizing parallel signal processing. The total number of rounding operations is also decreased from 24 to 8 (33.3 %). We experimentally demonstrate that it contributes to reducing total amount of the rounding noise in 5.

In detail, the 1st stage predicts X_{111} from all of the remaining groups as

$$\begin{aligned} x_{111}^{(1)}(\mathbf{m}) = x_{111}(\mathbf{m}) + R[&V_1 * H_1 * D_1 * x_{000}(\mathbf{m}) \\ &+ V_1 * H_1 * x_{001}(\mathbf{m}) \\ &+ V_1 * D_1 * x_{010}(\mathbf{m}) \\ &+ V_1 * x_{011}(\mathbf{m}) \\ &+ H_1 * D_1 * x_{100}(\mathbf{m}) \\ &+ H_1 * x_{101}(\mathbf{m}) \\ &+ D_1 * x_{110}(\mathbf{m})]. \end{aligned} \tag{24}$$

It includes convolution with multi-dimensional memory accessing. For example, the convolution '$V_1 * H_1 * D_1 *$ ' is defined as

$$\begin{aligned} V_1 * H_1 * D_1 * x_{000}(\mathbf{m}) = h_1^3 \{ & \\ x_{000}(m_1, m_2, m_3) + x_{000}(m_1^+, m_2, m_3) & \\ + x_{000}(m_1, m_2^+, m_3) + x_{000}(m_1^+, m_2^+, m_3) & \\ + x_{000}(m_1, m_2, m_3^+) + x_{000}(m_1^+, m_2, m_3^+) & \\ + x_{000}(m_1, m_2^+, m_3^+) + x_{000}(m_1^+, m_2^+, m_3^+) \} & \end{aligned} \tag{25}$$

where

$$m_1^+ = m_1 + 1, \quad m_2^+ = m_2 + 1, \quad m_3^+ = m_3 + 1. \tag{26}$$

In the 2nd lifting step, three predictions

$$\begin{aligned} x_{110}^{(2)}(\mathbf{m}) = x_{110}(\mathbf{m}) + R[&V_1 * H_1 * x_{000}(\mathbf{m}) \\ &+ V_1 * x_{010}(\mathbf{m}) + H_1 * x_{100}(\mathbf{m}) \\ &+ D_2 * x_{111}^{(1)}(\mathbf{m})] \end{aligned} \tag{27}$$

$$\begin{aligned} x_{101}^{(2)}(\mathbf{m}) = x_{101}(\mathbf{m}) + R[&V_1 * D_1 * x_{000}(\mathbf{m}) \\ &+ V_1 * x_{001}(\mathbf{m}) + D_1 * x_{100}(\mathbf{m}) \\ &+ H_2 * x_{111}^{(1)}(\mathbf{m})] \end{aligned} \tag{28}$$

$$\begin{aligned} x_{011}^{(2)}(\mathbf{m}) = x_{011}(\mathbf{m}) + R[&H_1 * D_1 * x_{000}(\mathbf{m}) \\ &+ H_1 * x_{001}(\mathbf{m}) + D_1 * x_{010}(\mathbf{m}) \\ &+ V_2 * x_{111}^{(1)}(\mathbf{m})] \end{aligned} \tag{29}$$

can be done simultaneously on a parallel signal processing platform since it is not necessary to wait for calculation results each other. Similarly, updating in the 3rd and 4th lifting steps are performed.

Note that there is no difference between the separable structure in Fig.5 and the non-separable structure in Fig.6 in respect of signals. It means that both of them are expressed with the same transfer function which is a product of 1D function. In this sense, the transform to be implemented is 'separable'. However, in respect of noise, those are different. The structure in Fig.6 is expected to have less rounding noise as it has less rounding operations. It is investigated in section 5.

4. Two-Dimensional (2D) Structures for 3D Wavelet Transform

Two-dimensional (2D) structures for the 3D integer wavelet transform is newly introduced.

4.1. Non-separable 2D Structures for 3D Transform

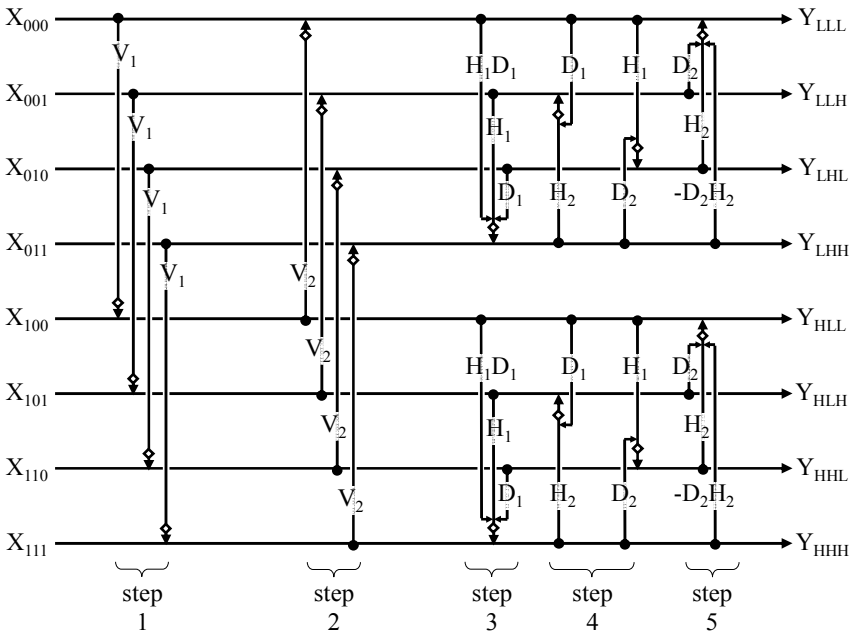

Figure 7. *Non-separable 2D structure 'Ns2D(1)' for 3D wavelet transform.*

Fig. 7 illustrates a newly introduced structure 'Ns2D(1)' for the 3D lifting wavelet transform. The 1st and the 2nd lifting steps are the same as those of the 'separable' structure in Fig. 5. However, the 3rd, 4th, 5th 6th lifting steps are implemented as the non-separable '2D' structure. It contributes to reduce hardware complexity comparing to 'Ns3D' in Fig. 6 since it does not use the 3D memory accessing.

Fig. 8 illustrates another variation 'Ns2D(2)' for the 3D transform. Unlike the structure in Fig. 7, the 1st, the 2nd and the 3rd lifting steps are implemented as the non-separable '2D' structure. Whereas the 4th and the 5th lifting steps are the same as those of the 'separable' structure in Fig. 5.

In brief, the structures appeared in this paper are expressed as

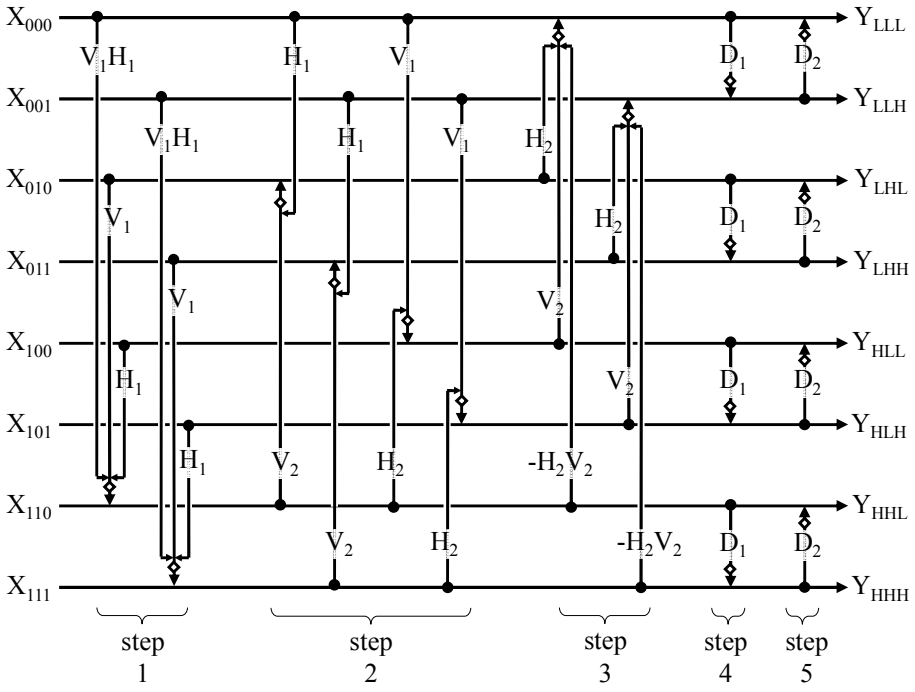

Figure 8. *Non-separable 2D structure 'Ns3D(2)' for 3D wavelet transform.*

$$\begin{cases} Sep3D & V_1V_2H_1H_2D_1D_2 & (Fig.5) \\ Ns3D & [V_1V_2H_1H_2D_1D_2] & (Fig.6) \\ Ns2D(1) & V_1V_2(H_1H_2D_1D_2) & (Fig.7) \\ Ns2D(2) & (V_1V_2H_1H_2)D_1D_2 & (Fig.8) \end{cases} \quad (30)$$

where [ ] in 'Ns3D' and ( ) in 'Ns2D' denote the non-separable 3D structure and the non-separable 2D structure.

4.2. Comparison of Structures

Table 1 summarizes the variations of the structure of the 3D integer wavelet transform. Unlike 'Ns3D', the newly introduced structures 'Ns2D(1) and 'Ns2D(2)' do not use inter-frame memory accessing which requires huge memory space. Instead, the total number of lifting steps is increased comparing to 'Ns3D'. The number of rounding operations is in the middle between 'Sep3D' and 'Ns3D'. In this paper, we compare the variations in (30) for various input signals from various aspects in 5.

Table 1. *Comparison of the structures.*

	Sep3D	Ns3D	Ns2D(1)	Ns2D(2)
Rounding operations	24	8	16	16
Lifting steps	6	4	5	5
Memory accessing	1D	3D	2D	2D

5. Experimental Results

In the following experiments, a set of MRI volumetric data in Fig. 9 provided by MATLAB is tested. Each frame has 256 $\times$ 256 pixels and each pixel is expressed with an 8 bit depth integer. Fig. 10 illustrates results of applying the 3D wavelet transform to the 8 frames of the MRI data. Note that each frequency band signals are normalized to the range of [0,255] for display purpose in this figure. In this paper, not only 1) variance of the noise in frequency domain and those in pixel domain, but also 2) the rate distortion curve in lossy coding mode and the entropy rate in lossless coding mode, 3) computational time of the transforms, and 4) feature comparison with other methods are investigated.

In this paper, the input signal is not limited to the MRI data like [34], but also a random 3D input signal is included. In addition, the 3D auto-regressive model expressed as

$$\begin{cases} x(n_1,n_2,n_3) = x'(n_1,n_2,n_3) + \rho \cdot x(n_1,n_2,n_3-1) \\ x'(n_1,n_2,n_3) = x''(n_1,n_2,n_3) + \rho \cdot x'(n_1,n_2-1,n_3) \\ x''(n_1,n_2,n_3) = w(n_1,n_2,n_3) + \rho \cdot x''(n_1-1,n_2,n_3) \end{cases} \quad (31)$$

is included into our experiments. Note that ρ is set to 0.9 in the experiments in this paper.

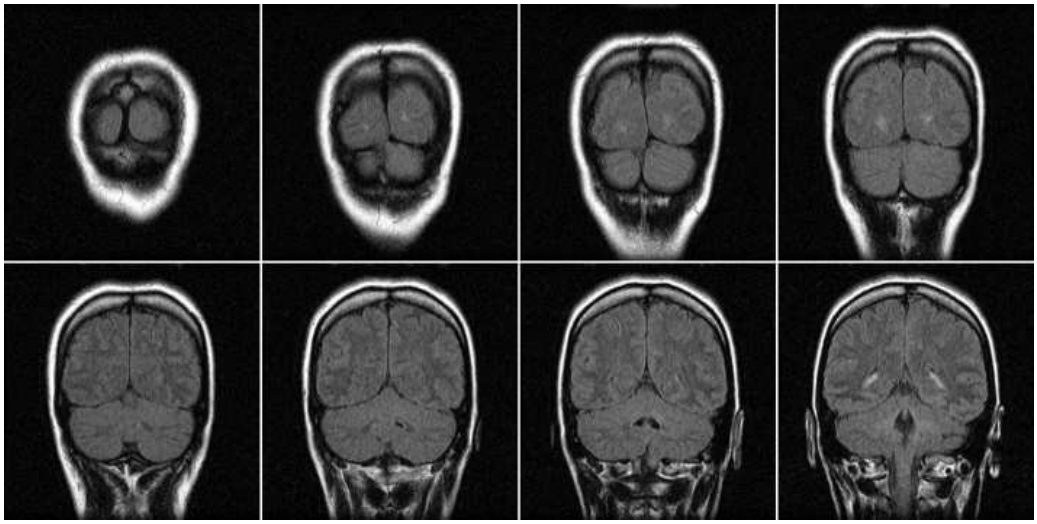

Figure 9. *Tested data set 'MRI'.*

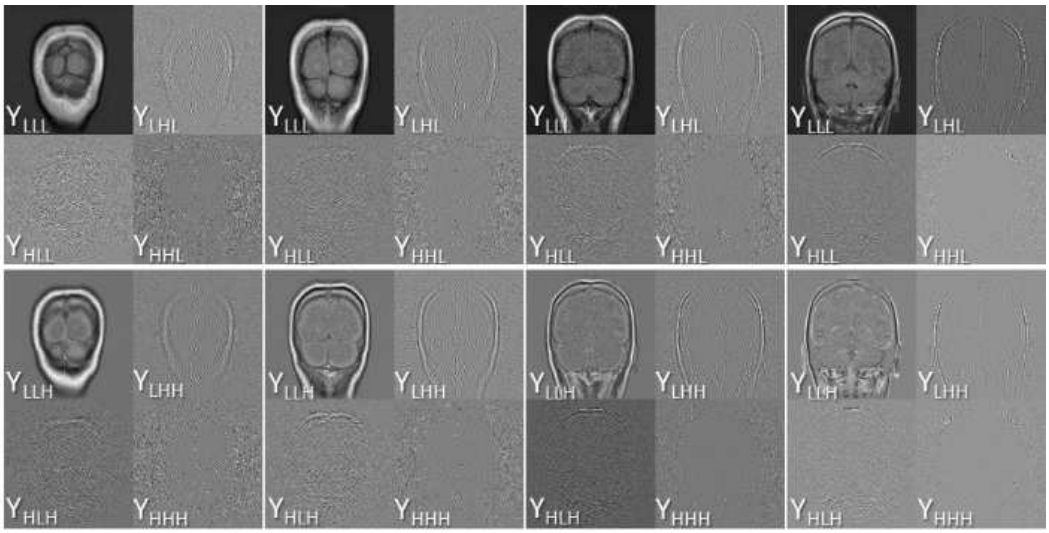

Figure 10. *Results of the 3D wavelet transform.*

5.1. Evaluation of Rounding Noise

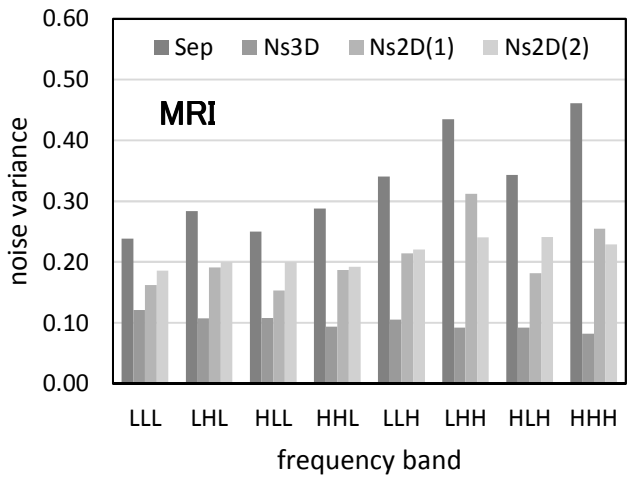

(a) MRI data

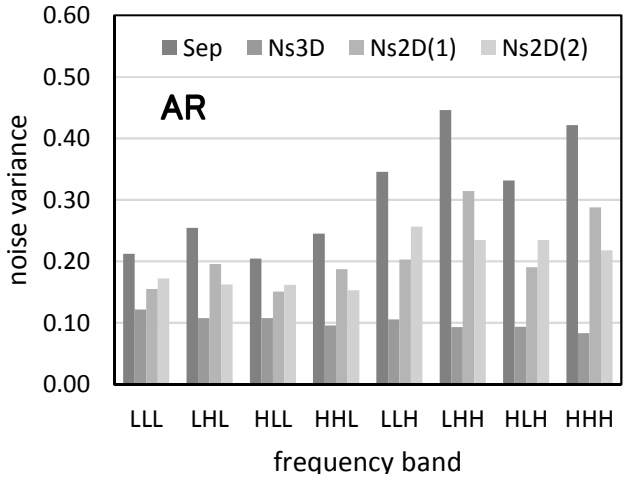

(b) AR model

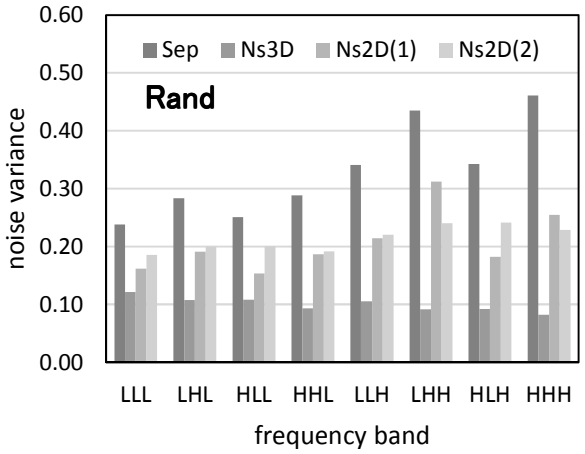

(c) Random input

Figure 11. *Rounding noise in each frequency band.*

Firstly, the structures summarized in table 1 are compared in respect of the rounding noise. Fig. 11(a), (b) and (c) indicate variance of the rounding noise in each frequency bands for MRI data, AR model, and random input, respectively. In all cases, variance of the noise in 'HHH' band of 'Ns3D' is 0.08. This is because the noise is not amplified. Since value of the rounding noise is in the range of [-0.5, 0.5], its variance is 1/12=0.08 just after each of the rounding operation. On the contrary, noise variance in 'LLL' band of 'Ns3D' is greater than 0.08. This is because multiple noise amplified though convolutions are summed up in Y_{LLL}. The highest noise variance is observed in 'LHH' band and 'HHH' band of 'Sep'. Noise variance is magnified approximately 0.45/0.08=5.6 times in those frequency bands in the separable structure in Fig. 5.

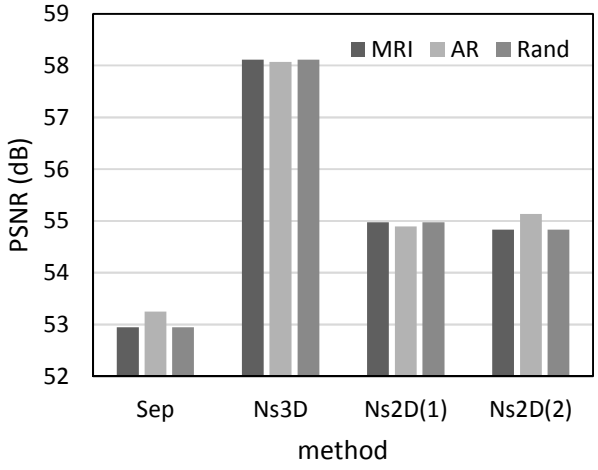

Figure 12. *Rounding noise in frequency domain.*

Fig. 12 illustrates averaged variance over all frequency bands in peak-signal to noise ratio (PSNR) defined as

$$PSNR = 10\log_{10}\frac{255^2}{\sigma^2} \quad (dB) \qquad (32)$$

where σ^2 denotes variance of the rounding error. It was observed that 'Ns3D' and 'Ns2D' increase PSNR by 5 (dB) and 2 (dB) respectively comparing to 'Sep'.

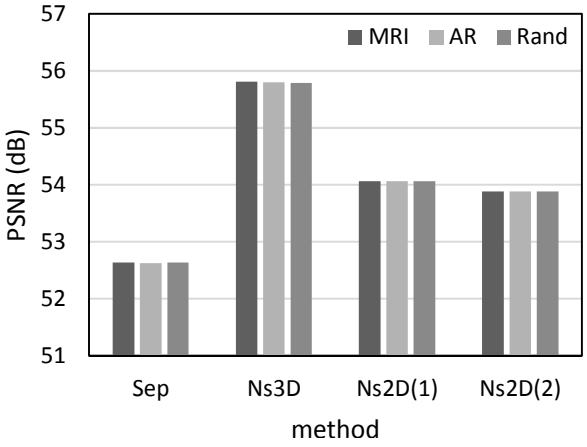

Figure 13. *Rounding noise in pixel domain.*

Fig.13 illustrates variance of the rounding noise in pixel domain. The input signal is transformed in forward without the rounding operation, and transformed in backward with the rounding operations. Variance of the rounding noise in this reconstructed signal is measured in this figure. Similarly to Fig. 13, 'Ns3D' is the best and 'Ns2D' is the second. There is no significant difference among input signals.

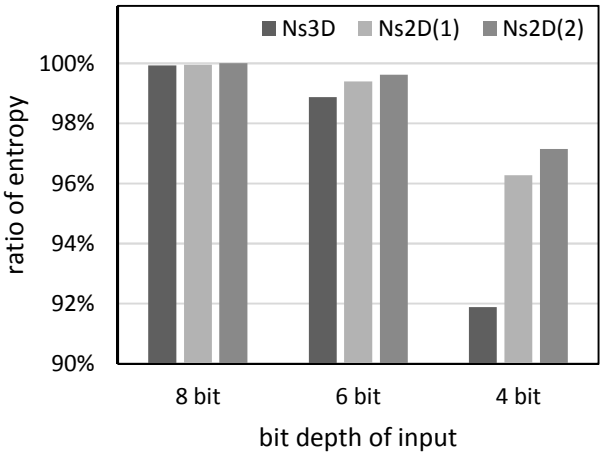

Figure 14. *Performance in lossless coding mode.*

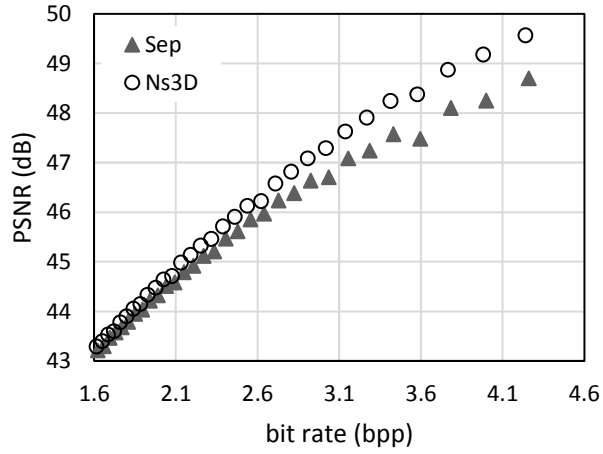

Figure 15. *Performance in lossy coding mode*

5.2. Evaluation of Coding Performance

Secondly, we investigate the entropy rate to evaluate lossless coding performance. Fig. 14 compares the structures in respect of lossless data compression rate for various bit depth of the input signal 'MRI'. The compression rate is defined as

$$\eta = \frac{H_{Str}}{H_{Sep}} \times 100 \quad (\%) \tag{33}$$

for $Str \in$ {Ns3D, Ns2D(1), Ns2D(2)} where H denotes the entropy rate in bit per pixel (bpp) averaged over all frequency band signals which approximates the average code length of the compressed data volume of the transformed signal.

According to Fig. 14, no significant difference was observed between the three methods for the original 8 bit depth signal. However, when the bit depth of the input signal is reduced to 4 (bit), the ratio of the entropy rate is decreased to 91.9 (%) and 96.2 (%) by 'Ns3D' and 'Ns2D(1)' respectively. Note that the bit depth of pixel values in the range of $[0, 2^B\text{-}1]$ is defined as B (bit). In conclusion, performance in lossless coding mode is improved by 8.1 (%) and 3.8 (%) by 'Ns3D' and 'Ns2D(1)' respectively for 4 bit depth 'MRI' volumetric data.

Fig.15 indicates rate-distortion curve of 'Sep' and that of 'Ns3D'. The horizontal axis and the vertical axis indicate entropy rate and PSNR of the reconstructed signal, respectively. In this experiment, quantization is introduced just after the forward transform. These curves indicate performance of the methods in lossy coding mode. It was observed that 'Ns3D' is higher than 'Sep' by approximately 1.5 (dB) at 6.5 (bpp). In conclusion, superiority of the non-separable structure over the conventional separable structure was observed.

5.3. Evaluation of Computational Time

Thirdly, computational time of the structures for the 3D transform was investigated. Table 2 summarizes computational time of 'Sep3D', 'Ns3D', 'Ns2D(1)' and 'Ns2D(2)', respectively. These algorithms were performed with MATLAB program on Dell Inspiron 580 PC, Intel Core i3-550 Processor 3.2 GHz, 4GB RAM on Windows 7.

According to the table, it was observed that 'Ns3D' is the fastest. Both of 'Ns2D(1)' and 'Ns2D(2)' are almost the same, and the second in computational speed. Those are faster than 'Sep3D' by 19 (ms). The result confirms that less lifting steps mean faster computation of the transform.

Table 2. *Comparison of computational time.*

	Sep3D	**Ns3D**	**Ns2D(1)**	**Ns2D(2)**
Computational time	120.7 ms	97.9 ms	101.3 ms	101.4 ms

5.4. Comparison with Other Methods

Fourthly, the methods investigated in this paper are compared to other conventional methods. Table 3 summarizes features of those methods. The well-known international standards 'JPEG', 'JPEG-LS' and 'JPEG 2000' performs lossless coding. However, those are limited to 2D signals. Other methods such as 'Huffyuv' and its improved version 'Lagarith' can be applied to 3D signals. However those do not support the 'scalability'. This feature makes it possible to analyze the input signal in frequency domain. Therefore this paper focused on 'Sep3D', 'Ns3D' and 'Ns2D'. Among these methods, it was found that 'Ns3D' has the minimum lifting steps, the minimum rounding noise and the minimum computational time.

Table 3. *Comparison with other methods*

	JPEG	**JPEG LS**	**Huffyuv**	**Lagarith**	**JPEG 2000**	**Sep3D**	**Ns3D**	**Ns2D**
Input signal	2D	2D	3D	3D	2D	3D	3D	3D
Entropy coding	Arithmetic coding	Golumb-Rice	Huffman coding	Huffman +Run Length +Arithmetic	EBCOT	EBCOT	EBCOT	EBCOT
Transform or prediction	DPCM	adaptive prediction	DPCM	median prediction	(5,3) wavelet	(5,3) wavelet	(5,3) wavelet	(5,3) wavelet
Scalability	N.A.	N.A.	N.A.	N.A.	available	available	available	available
Frequency analysis	N.A.	N.A.	N.A.	N.A.	available	available	available	available
Lifting steps	---	---	---	---	---	many	minimum	reduced
Memory accessing	1D	2D	1D	1D	1D	1D	3D	2D

6. Conclusions

A 3D integer lifting wavelet transform with reduced amount of rounding noise was proposed. Non-separable multi-dimensional lifting structures were introduced to decrease the total number of lifting steps as well as the rounding operations. It was experimentally observed that the non-separable 3D structure increases PSNR by 5 (dB) in frequency for MRI, AR model and random input signals. It was also observed that the non-separable 2D structure increases PSNR by 2 (dB) without using inter-frame memory accessing. Those PSNR improvements were also observed in rate-distortion curves at high bit rates in lossy coding mode. In lossless coding mode, data compression performance is improved for low bit depth input images. Computational time was also improved by the proposed method.

Acknowledgements

This work was supported by JSPS KAKENHI Grant Number 26289117.

References

[1] Chao He, Dong, J., Zheng, Y. F., Zhigang Gao: Optimal 3-D coefficient tree structure for 3-D wavelet video coding, IEEE Trans. Circuits and Systems for Video Technology, vol.13, Issue 10, pp.961-972 (2003)

[2] Aggoun, A.: Compression of 3D integral images using 3D wavelet transform, IEEE Journal of Display Technology, vol.7, Issue 11, pp.586-592 (2011)

[3] B. Penna, T. Tillo, E. Magli, G. Olmo: Progressive 3-D coding of hyperspectral images based on JPEG 2000, IEEE Geoscience, Remote Sensing Letters, vol.3, issue 1, pp.125-129 (2006)

[4] Z. Xiong, X. Wu, S. Cheng, J. Hua:Lossy-to-lossless compression of medical volumetric data using three-dimensional integer wavelet transforms, IEEE Trans Medical Imaging, 22 (3), pp.459-70 (2003)

[5] ISO / IEC FCD 15444-1, Joint Photographic Experts Group: JPEG 2000 image coding system, (March 2000)

[6] Skodras, A., Christopoulos, C., Ebrahimi, T.: The JPEG 2000 still image compression standard. IEEE Signal ProcessingMagazine, 18, pp.36-58 (2001)

[7] A. Descampe, F. Devaux, G. Rouvroy, J. D. Legat, J. J. Quisquater and B. Macq: A flexible hardware JPEG 2000 decoder for digital cinema, IEEE Trans. Circuits and Systems for Video Technology, vol. 16, issue 11, pp.1397-1410 (Nov. 2006)

[8] Kaneko, K., Ohta, N.: 4K applications beyond digital cinema. In: Proc. Int. Conf. Virtual Syst. Multimedia, pp. 133-136 (2010)

[9] C. Chrysafis, A. Ortega: Line-based, reduced memory, wavelet image compression, IEEE Trans. Image Processing, vol.9, no.3, pp.378-389 (March 2000)

[10] G. Shi, W. Liu, Li Zhang and Fu Li: An efficient folded architecture for lifting-based discrete wavelet transform, IEEE Trans. Circuits, Systems II express briefs, vol.56, no.4, pp.290-294 (April 2009)

[11] Bing-Fei Wu, Chung-Fu Lin: A high-performance and memory-efficient pipeline architecture for the 5/3 and 9/7 discrete wavelet transform of JPEG 2000 codec, IEEE Trans. Circuits and Systems for Video Technology, vol.15, no.12, pp.1615-1628 (Dec. 2005)

[12] Siqi Li: The regularity of wavelet transform with the high order vanishing moments, Proc. IEEE International Conf. Measurement, Information and Control (ICMIC), vol.2, pp.1358-1361 (2013)

[13] Vetterli, M., Herley, C.: Wavelets and filter banks: theory and design," IEEE Trans. Signal Processing, vol.40, Issue 9, pp.2207-2232 (1992)

[14] Zhang, Y., Bull, D.R., Reinhard, E.: Perceptually lossless high dynamic range image compression with JPEG 2000, Proc. IEEE International Conference on Image Processing, pp.1057-1060 (2012)

[15] Shih, Y.S., Zhang, W.C., Sheng, H., et.al.: Bio-inspired JPEG XR CODEC design for lossless HDR biomedical image, Proc. International Computer Symposium, pp. 148-153 (2010)

[16] N. Zhang, X. Wu: Lossless compression of color mosaic images, IEEE Trans. on Image Processing, vol.15, no.6, pp.1379-1388 (June 2006)

[17] PengweiHao,Qingyun Shi: Reversible Integer KLT for progressive-to-lossless compression of multiple component images, IEEE International Conf. on Image Processing (ICIP), vol. 1, pp. 633-636 (Sept. 2003)

[18] M. Iwahashi, M. Ogawa, H. Kiya: Avoidance of singular point in integer orthonormal transform for lossless coding, IEEE Trans. on Signal Processing, vol.60, no.5, pp.2648-2653 (May 2012)

[19] S.Poomrittigul, M. Ogawa, M.Iwahashi, H.Kiya: Reversible color transform for Bayer color filter array images, APSIPA Transactions on Signal and Information Processing, vol.2, pp.1-10 (Sept. 2013)

[20] H. S. Malvar, G. J. Sullivan, S. Srinivasan: Lifting-based reversible color transformations for image compression, SPIE vol. 7073 (2008)

[21] V. Britanak, P. Yip and K. R. Rao: Discrete cosine and sine transform, general properties, fast algorithm and integer approximations, Academic Press (2007)

[22] A. Benazza-Benyahia, J. C. Pesquet and M. Hamdi: Vector-lifting schemes for lossless coding and progressive archival of multispectral images, IEEE Trans. on Geoscience & Remote Sensing, vol.40, issue 9, pp.2011-2024 (Sep. 2002)

[23] S. Chokchaitam, M. Iwahashi: Lossless lossy image compression based on non-separable two-dimensional L-SSKF, IEEE International Symposium, Circuits and Systems (ISCAS), pp.421-424 (May 2002)

[24] D. S. Taubman: Adaptive, non-separable lifting transforms for image compression, IEEE International Conference on Image Processing (ICIP), vol.3, pp.772-776 (1999)

[25] S. Fukuma, M. Iwahashi and N. Kambayashi: Adaptive multi-channel prediction for lossless scalable coding, IEEE International Symposium on Circuits and Systems (ISCAS), no.IV, pp. 467-470 (May 1999)

[26] M. Kaaniche, J. C. Pesquet, A. B. Benyahia, B. P. Popescu: Two-dimensional non separable adaptive lifting scheme for still and stereo image coding, IEEE International Conference on Acoustics, Speech, and Signal Processing (ICASSP), pp.1298-1301 (March 2010)

[27] M. Kaaniche, B. P. Popescu, A. B. Benyahia, J.C. Pesquet: Adaptive lifting scheme with sparse criteria for image coding, EURASIP Journal on Advances in Signal Processing: Special Issue on New Image and Video Representations Based on Sparsity, vol. 2012, pp.1-22 (Jan.2012)

[28] T. Yoshida, T. Suzuki, S. Kyochi, M. Ikehara: Two dimensional non-separable adaptive directional lifting structure of discrete wavelet transform, IEEE International Conference on Acoustics, Speech and Signal Processing (ICASSP), pp.1529-1532 (May 2011)

[29] T. Yoshida, T. Suzuki, S. Kyochi, M. Ikehara: Two dimensional non-separable adaptive directional lifting structure of discrete wavelet transform, IEICE Trans. Fundamentals, vol.E94-A, no.10, pp.1920-1927 (Oct. 2011)

[30] M. Iwahashi, H. Kiya: Non separable 2D factorization of separable 2D DWT for lossless image coding, IEEE International Conference Image Processing (ICIP), pp.17-20 (Nov. 2009)

[31] M. Iwahashi, H. Kiya: A New lifting structure of non separable 2D DWT with compatibility to JPEG 2000, IEEE International Conference on Acoustics, Speech, and Signal Processing (ICASSP), IVMSP, P9.7, pp.1306-1309 (March 2010)

[32] T. Strutz, I. Rennert, Two-dimensional integer wavelet transform with reduced influence of rounding operations, EURASIP Journal on Advances in Signal Processing, vol.2012, 2012:75, ISSN:1687-6180 (April 2012)

[33] M. Iwahashi, H. Kiya: Discrete wavelet transforms: Non separable two dimensional discrete wavelet transform for image signals, ISBN 980-953-307-580-3, InTech (2013)

[34] M. Iwahashi, T. Orachon, H. Kiya: Three dimensional discrete wavelet transform with deduced number of lifting steps, IEEE International Conference on Image Processing (ICIP), no.WA.L4, pp.1651-1654 (Sept. 2013)